Printed ISSN 1330–0016
Online ISSN 1333–9133
CD ISSN 1333–8390
CODEN FIZBE7

INTENSE TWO-STEP CASCADES AND γ-DECAY SCHEME OF THE ^{118}Sn COMPOUND NUCLEUS

JAROSLAV HONZÁTKO[a], VALERY A. KHITROV[b], CVETAN PANTELEEV[b], ANATOLY M. SUKHOVOJ[b] and IVO TOMANDL[a]

[a]*Nuclear Physics Institute, CZ-25068 Řež near Prague, Czech Republic*

[b]*Frank Laboratory of Neutron Physics, Joint Institute for Nuclear Research, 141980 Dubna, Russia*

Received 10 February 2005; Revised manuscript received 5 December 2006
Accepted 13 December 2006 Online 23 February 2007

Transition energies and intensities of 453 two-step cascades following thermal neutron capture in ^{117}Sn have been measured. The data allowed us to considerably extend previous decay scheme of the ^{118}Sn nucleus and to achieve more precise results. Autocorrelation analysis of the excitation spectrum of intermediate levels of the most intense cascades allowed us to determine most probable period of their regularity. Besides, analysis showed the impossibility to reproduce quantitatively the total cascade intensities taking into account only excitations of the fermion type. The results lead to the conclusion that the excitations of vibrational type considerably influence the cascade γ-decay process in ^{118}Sn almost up to the neutron separation energy S_n.

PACS numbers: 25.40.LW, 27.60.+j UDC 539.172.4
Keywords: thermal neutron capture in ^{117}Sn, two-step cascades, decay scheme of ^{118}Sn nucleus

1. Introduction

The understanding of processes occurring in nuclei and precise determination of their properties (e.g., decay schemes, neutron cross-sections, etc.) requires their detailed experimental study in wide intervals of excitation energy in stable and radioactive nuclei.

This work presents investigations of the two-step γ-cascades following thermal neutron capture in the target nucleus ^{117}Sn. The energies of γ-transitions and intensities of the strongest 453 cascades exciting 303 levels in the ^{118}Sn compound

nucleus were determined in the energy interval almost up to the neutron separation energy, S_n.

2. Experiment

The experiment was performed at the LWR-15 reactor in Řež. The experimental arrangement used in the measurements is described in Ref. [1]. The target enriched in ^{117}Sn to more than 91% was used in the experiment.

The sum coincidence spectrum of the two-step cascades measured in the experiment is presented in Fig. 1. Using this spectrum, 8 intensity distributions for the cascades terminating at low-lying levels with $E_f < 2.41$ MeV and $E_f = 2.74$ MeV of ^{118}Sn were derived. Each two-step cascade in a spectrum is presented by a pair of peaks with equal areas and widths [2]. Energy resolution in each of these distributions varies from 1.9 keV at their ends up to 3 keV in their centres. That resolution and the achieved statistics of coincidences, with a low and almost constant background at any energy in these spectra, provided the detection threshold $\simeq 0.6\times10^{-4}$ events per decay for the cascades to the ground state and $(2-5)\times10^{-4}$ events per decay for the cascades to the higher-lying levels.

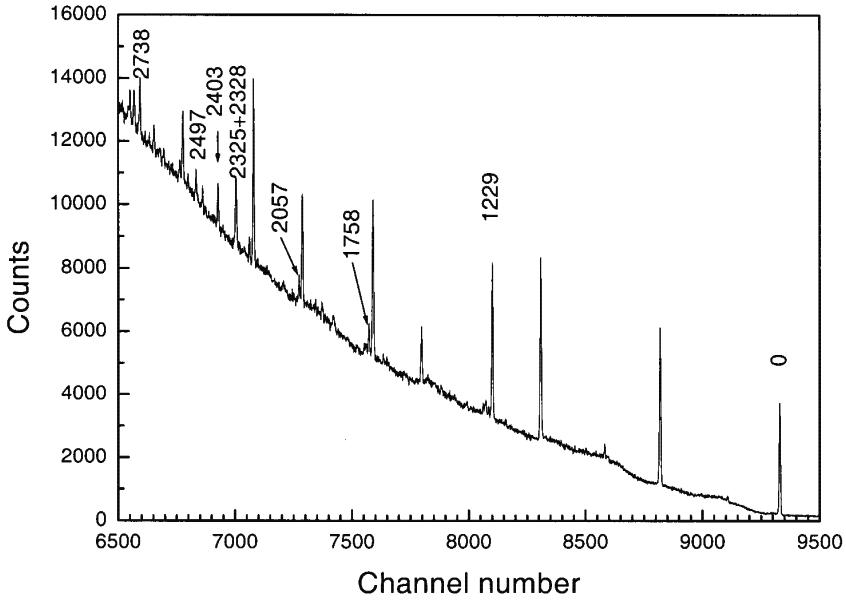

Fig. 1. The part of the sum coincidence spectrum for the target enriched in ^{117}Sn. *Full-energy peaks are labelled with the energy (in* keV*) of the final cascade levels.*

The spectrum in Fig. 1 is very specific as compared with those of other nuclei studied by us earlier. It has single-escape and double-escape peaks corresponding not only to one cascade transition but also to both transitions simultaneously.

Thus, the cascades to the ground and first excited states of ^{118}Sn create in the sum coincidence spectrum four well expressed additional peaks shifted by 511 keV and its multiples.

2.1. Sources of background and its influence on the quality of spectroscopic data

The main and strongest source of background in the present experiment is the incomplete absorption of energy of the cascade quanta in both detectors. Although the area of this background under any peak may be determined with a very high accuracy from the spectrum presented in Fig. 1, its subtraction strongly increases the noise line as shown in Fig. 2. Only this circumstance has limited the accuracy of the spectroscopy data shown in Table 1.

Since we used a highly-enriched target of ^{117}Sn, the contribution of the isotopes ^{115}Sn and ^{119}Sn in the capture spectra does not exceed 5% of the captures due to the investigated isotope ^{117}Sn. For this reason and because of the very high statistics, the cascades from the ^{116,120}Sn isotopes did not interfere in the analysis of the coincidence spectra and do not appear in Table 1. High resolution of the experiment and large spacing of low-lying levels in ^{118}Sn also exclude the possibility to misinterpret the peaks of cascades involving the escape of one or two annihilation quanta of the gamma-transitions of high-energy cascades.

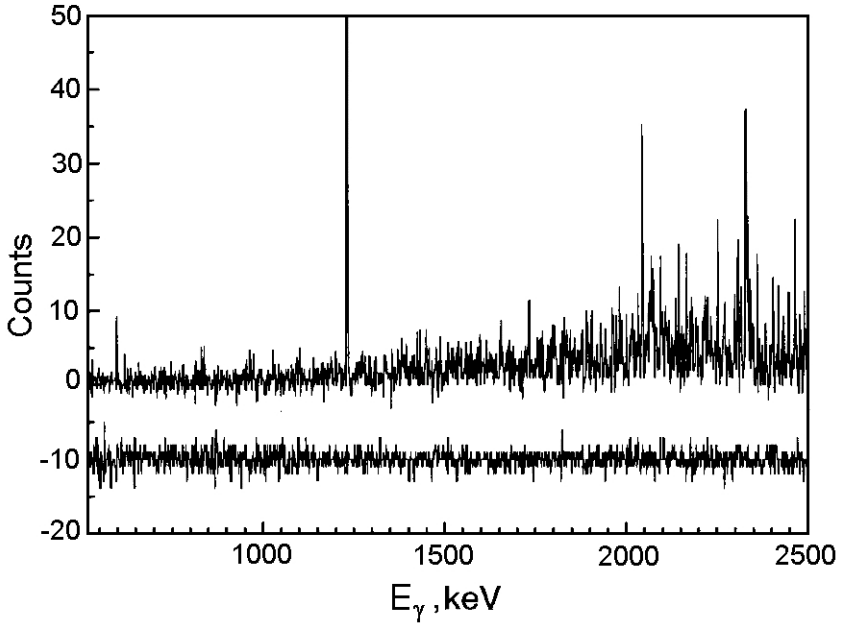

Fig. 2. The part of intensity distribution of the two-step cascades terminating at the ground state of ^{118}Sn. *The background spectrum with the close sum energy presented for the comparison is shifted down by 10 counts.*

TABLE 1. A list of absolute intensities (per 10^2 decays), $i_{\gamma\gamma}$, of measured two-step cascades, and energies, E_1 and E_2, of the cascade transitions. E_i are energies of the intermediate levels. All energies are in keV.

E_1	E_i	E_2	$i_{\gamma\gamma}$	E_1	E_i	E_2	$i_{\gamma\gamma}$
8095.5	1230.8(1)	1230.8	0.366(18)	5813.2	3513.1(3)	3513.1	0.018(5)
7567.3	1759.0(1)	529.3	0.026(4)			2283.4	0.024(7)
7282.4	2043.9(3)	2043.9	0.054(8)	5739.7	3586.6(2)	1260.7	0.026(7)
		814.2	0.075(7)	5724.5	3601.8(3)	3601.8	0.048(7)
7268.2	2058.1(1)	828.4	0.444(13)			2372.1	0.020(7)
6997.4	2328.9(3)	2328.9	0.069(10)	5688.6	3637.7(5)	3637.7	0.029(7)
		1099.2	0.243(13)			1311.8	0.047(6)
6922.9	2403.4(9)	2403.4	0.024(5)	5630.2	3696.1(2)	2466.4	0.046(8)
		1173.7	0.104(8)	5626.3	3700.0(6)	3700.0	0.037(7)
6828.1	2498.2(1)	1268.5	0.366(13)			2470.3	0.038(8)
6750.6	2575.7(6)	2575.7	0.013(5)			1374.1	0.129(8)
6747.2	2579.1(3)	2579.1	0.024(7)			962.0	0.123(10)
6648.3	2678.0(2)	2678.0	0.365(24)	5563.3	3763.0(3)	2533.3	0.494(23)
		1448.3	0.350(11)			1720.1	0.046(4)
		919.7	0.030(5)			1437.1	0.073(7)
6587.4	2738.9(3)	2738.9	0.051(8)	5478.6	3847.7(6)	3847.7	0.038(7)
		1509.2	0.104(8)			2618.0	0.031(10)
6421.5	2904.8(2)	2904.8	0.646(39)			1521.8	0.046(7)
		1675.1	0.217(11)	5469.1	3857.2(3)	3857.2	0.106(12)
		861.9	0.014(3)			2627.5	0.028(10)
6268.3	3058.0(3)	3058.0	0.029(7)	5459.8	3866.5(6)	2636.8	0.041(10)
6192.2	3134.1(3)	1904.4	0.026(7)			1540.6	0.049(7)
6188.2	3138.1(1)	1908.4	0.044(7)	5443.0	3883.3(1)	1557.4	0.349(13)
6167.5	3158.8(1)	3158.8	0.128(13)	5436.9	3889.4(1)	3889.4	0.170(15)
6110.3	3216.0(11)	3216.0	0.098(12)	5382.0	3944.3(4)	3944.3	0.056(8)
		1986.3	0.164(13)			2714.6	0.047(11)
		1173.1	0.122(8)	5330.7	3995.6(3)	2765.9	0.031(10)
		890.1	0.158(12)			1952.7	0.018(3)
6096.5	3229.8(8)	3229.8	0.214(18)	5297.1	4029.2(1)	1291.2	0.174(9)
		2000.1	0.034(7)	5280.9	4045.4(2)	2815.7	0.078(13)
6065.6	3260.7(1)	3260.7	0.144(15)	5216.9	4109.4(5)	2879.7	0.586(31)
6055.2	3271.1(1)	3271.1	0.552(28)			2066.5	0.013(3)
6052.4	3273.9(2)	2044.2	0.031(7)	5208.6	4117.7(2)	4117.7	0.445(24)
6016.6	3309.7(6)	3309.7	0.021(5)			2888.0	0.635(31)
		2080.0	0.070(8)			2074.8	0.009(3)
5986.1	3340.2(4)	3340.2	0.037(8)	5193.1	4133.2(3)	4133.2	0.062(10)
		2110.5	0.024(7)			2903.5	0.024(10)
5972.3	3354.0(3)	2124.3	0.168(16)	5134.9	4191.4(6)	4191.4	0.016(5)
		1311.1	0.017(3)			2961.7	0.259(20)
5969.8	3356.5(2)	3356.5	0.053(8)			1865.5	0.069(7)
		2126.8	0.182(16)	5099.3	4227.0(3)	4227.0	0.080(12)
		1313.6	0.014(3)			2997.3	0.217(22)
5961.3	3365.0(1)	3365.0	0.096(12)	5037.9	4288.4(1)	3058.7	0.181(20)
5951.3	3375.0(12)	3375.0	0.058(8)	5025.3	4301.0(3)	4301.0	0.024(7)
		2145.3	0.029(7)			3071.3	0.044(13)
		1049.1	0.056(9)	5014.1	4312.2(7)	3082.5	0.040(11)
5944.2	3382.1(1)	3382.1	0.163(15)			2269.3	0.014(3)
5900.3	3426.0(3)	1100.1	0.029(8)			1986.3	0.106(8)
5866.7	3459.6(4)	1133.7	0.025(9)			1574.2	0.102(8)
5862.5	3463.8(7)	3463.8	0.056(8)	4993.3	4333.0(5)	4333.0	0.018(5)
		2234.1	0.032(7)			3103.3	0.035(11)
		1420.9	0.055(4)	4972.5	4353.8(5)	4353.8	0.069(10)
		1137.9	0.057(9)			3124.1	0.395(28)

Table 1. (cont.)

E_1	E_i	E_2	$i_{\gamma\gamma}$	E_1	E_i	E_2	$i_{\gamma\gamma}$
		2595.5	0.059(8)	4509.6	4816.7(5)	3058.4	0.031(8)
		2310.9	0.056(5)			2078.7	0.034(10)
		2296.9	0.076(13)	4496.7	4829.6(1)	4829.6	0.098(13)
4949.4	4376.9(7)	4376.9	0.011(5)	4492.0	4834.3(6)	3604.6	0.063(10)
		2051.0	0.066(8)			2508.4	0.084(11)
		1638.9	0.029(8)	4482.0	4844.3(2)	4844.3	0.075(12)
4922.0	4404.3(3)	4404.3	0.058(10)	4477.7	4848.6(3)	4848.6	0.013(5)
		2361.4	0.038(4)			3618.9	0.029(8)
4919.0	4407.3(6)	4407.3	0.050(10)			2110.6	0.129(10)
		3177.6	0.393(30)	4456.8	4869.5(5)	4869.5	0.029(8)
		2081.4	0.033(8)			3639.8	0.037(8)
4915.8	4410.5(3)	2652.2	0.027(8)	4451.7	4874.6(2)	4874.6	0.094(13)
		2367.6	0.028(4)	4446.7	4879.6(3)	4879.6	0.038(8)
4891.0	4435.3(4)	3205.6	0.031(11)			3121.3	0.036(8)
		2677.0	0.023(7)	4432.8	4893.5(1)	4893.5	0.080(12)
4836.5	4489.8(1)	4489.8	0.218(18)	4415.5	4910.8(6)	4910.8	0.011(5)
4824.7	4501.6(6)	3271.9	0.029(10)			3681.1	0.050(10)
		2743.3	0.019(8)			2584.9	0.199(15)
4789.5	4536.8(5)	4536.8	0.211(18)			2507.6	0.058(9)
		3307.1	0.038(10)	4406.6	4919.7(1)	2862.8	0.190(21)
		2778.5	0.061(9)	4402.9	4923.4(3)	2880.5	0.046(5)
		2493.9	0.021(4)			2520.2	0.025(8)
4781.3	4545.0(6)	4545.0	0.117(13)	4384.6	4941.7(3)	2898.8	0.017(4)
		3315.3	0.037(10)			2615.8	0.036(10)
		2502.1	0.030(4)	4370.5	4955.8(5)	4955.8	0.014(5)
		2488.1	0.055(11)	4344.8	4981.5(2)	4981.5	0.011(5)
		2141.8	0.044(6)			3751.8	0.047(10)
4765.6	4560.7(3)	4560.7	0.174(16)			2924.6	0.066(13)
		3331.0	0.081(11)			2655.6	0.036(10)
		2802.4	0.129(12)	4325.3	5001.0(3)	5001.0	0.026(7)
		2503.8	0.126(15)	4295.3	5031.0(4)	5031.0	0.026(8)
4731.8	4594.5(3)	4594.5	0.030(7)	4282.9	5043.4(3)	5043.4	0.014(5)
		3364.8	0.024(10)			3813.7	0.054(10)
4700.9	4625.4(2)	2568.5	0.059(11)	4250.6	5075.7(3)	5075.7	0.032(8)
4685.6	4640.7(3)	2583.8	0.048(11)	4248.0	5078.3(9)	5078.3	0.046(10)
4658.9	4667.4(3)	2610.5	0.040(11)			3320.0	0.030(8)
4653.7	4672.6(2)	4672.6	0.058(10)			3035.4	0.009(4)
4627.4	4698.9(4)	4698.9	0.021(7)	4236.0	5090.3(4)	5090.3	0.070(10)
4614.5	4711.8(4)	4711.8	0.018(7)			3860.6	0.109(13)
4602.4	4723.9(9)	4723.9	0.024(7)			3332.0	0.015(6)
		3494.2	0.052(11)			3047.4	0.034(5)
		2681.0	0.009(4)	4217.2	5109.1(5)	5109.1	0.014(5)
4584.3	4742.0(3)	4742.0	0.024(7)	4206.7	5119.6(4)	5119.6	0.014(5)
4556.8	4769.5(6)	3539.8	0.028(8)			3076.7	0.031(5)
		2443.6	0.122(11)			3062.7	0.050(12)
		2366.3	0.126(10)			2793.7	0.041(13)
4553.5	4772.8(5)	4772.8	0.034(8)	4201.7	5124.6(5)	3894.9	0.038(10)
		3543.1	0.035(8)			2386.6	0.093(10)
		2729.9	0.017(4)	4184.5	5141.8(8)	3912.1	0.124(13)
		2446.9	0.035(9)			3383.5	0.019(8)
4547.6	4778.7(3)	3020.4	0.050(8)			2815.9	0.030(13)
		2735.8	0.017(4)			2738.6	0.049(9)
		2721.8	0.049(10)	4163.5	5162.8(8)	5162.8	0.050(8)
4523.4	4802.9(5)	3573.2	0.026(8)			2836.9	0.039(13)
		2760.0	0.011(4)			2759.6	0.024(9)
		2477.0	0.029(9)	4144.8	5181.5(3)	3124.6	0.065(12)

Table 1. (cont.)

E_1	E_i	E_2	$i_{\gamma\gamma}$	E_1	E_i	E_2	$i_{\gamma\gamma}$
		2778.3	0.047(9)	3588.7	5737.6(8)	5737.6	0.168(13)
4124.9	5201.4(9)	5201.4	0.048(8)			3411.7	0.031(9)
		3971.7	0.034(8)	3568.3	5758.0(5)	5758.0	0.019(5)
		3158.5	0.015(4)			3432.1	0.043(9)
4105.8	5220.5(2)	5220.5	0.029(7)	3552.9	5773.4(2)	4543.7	0.064(10)
4093.2	5233.1(3)	3190.2	0.024(4)	3535.5	5790.8(3)	5790.8	0.021(5)
		3176.2	0.046(11)	3502.6	5823.7(3)	5823.7	0.016(5)
4082.1	5244.2(3)	5244.2	0.045(8)	3496.3	5830.0(2)	4600.3	0.089(13)
		4014.5	0.020(10)	3486.7	5839.6(7)	5839.6	0.030(7)
4073.0	5253.3(4)	5253.3	0.014(5)			4609.9	0.031(8)
4064.0	5262.3(3)	5262.3	0.024(7)	3475.7	5850.6(4)	5850.6	0.051(8)
4051.4	5274.9(5)	5274.9	0.102(12)			4620.9	0.083(11)
		3232.0	0.022(4)			3807.7	0.035(4)
4025.5	5300.8(4)	4071.1	0.032(10)	3465.2	5861.1(3)	4631.4	0.034(8)
4003.3	5323.0(5)	5323.0	0.142(15)	3456.1	5870.2(3)	5870.2	0.018(5)
		3564.7	0.043(8)	3451.5	5874.8(2)	3831.9	0.022(4)
		2997.1	0.050(11)	3448.3	5878.0(4)	3835.1	0.011(4)
3996.8	5329.5(3)	5329.5	0.046(8)	3444.6	5881.7(2)	4652.0	0.073(11)
		4099.8	0.034(10)	3434.2	5892.1(6)	5892.1	0.080(10)
3983.0	5343.3(6)	5343.3	0.093(12)			4662.4	0.032(10)
		4113.6	0.057(10)	3428.9	5897.4(3)	5897.4	0.021(5)
		3300.4	0.010(4)	3422.9	5903.4(2)	5903.4	0.056(8)
3978.1	5348.2(8)	4118.5	0.050(10)	3419.0	5907.3(12)	5907.3	0.016(5)
		3589.9	0.025(8)			4677.6	0.023(8)
		3305.3	0.018(4)	3407.3	5919.0(4)	5919.0	0.030(7)
		3022.3	0.068(11)			4689.3	0.041(10)
3967.0	5359.3(6)	4129.6	0.020(8)	3401.1	5925.2(6)	4695.5	0.023(10)
3958.9	5367.4(1)	5367.4	0.077(10)	3392.6	5933.7(6)	5933.7	0.046(8)
3929.6	5396.7(5)	5396.7	0.094(12)			4704.0	0.043(10)
		3339.8	0.050(11)	3387.8	5938.5(5)	4708.8	0.029(10)
3917.3	5409.0(5)	4179.3	0.024(8)	3380.2	5946.1(3)	4716.4	0.043(10)
3902.0	5424.3(7)	4194.6	0.023(10)	3358.0	5968.3(4)	4738.6	0.035(10)
		3666.0	0.025(8)	3351.9	5974.4(2)	5974.4	0.045(8)
		3367.4	0.057(14)	3331.4	5994.9(12)	5994.9	0.035(7)
		3021.1	0.030(7)			3952.0	0.012(4)
3879.3	5447.0(3)	5447.0	0.085(10)	3322.1	6004.2(2)	6004.2	0.064(10)
		3121.1	0.036(11)			4774.5	0.052(10)
3823.8	5502.5(3)	5502.5	0.030(7)	3303.9	6022.4(3)	4792.7	0.054(11)
		3459.6	0.011(3)	3293.4	6032.9(1)	6032.9	0.029(7)
3808.8	5517.5(3)	5517.5	0.099(12)			4803.2	0.037(10)
		4287.8	0.061(10)	3284.4	6041.9(3)	4812.2	0.037(10)
3801.0	5525.3(5)	5525.3	0.205(16)	3278.2	6048.1(1)	6048.1	0.016(7)
		4295.6	0.020(10)			4818.4	0.038(10)
3777.1	5549.2(11)	5549.2	0.018(5)			3722.2	0.030(9)
		4319.5	0.024(10)	3265.3	6061.0(3)	6061.0	0.037(8)
3767.5	5558.8(7)	4329.1	0.020(10)	3252.7	6073.6(4)	6073.6	0.019(7)
3760.5	5565.8(5)	5565.8	0.013(5)	3245.5	6080.8(1)	6080.8	0.062(10)
3736.7	5589.6(2)	5589.6	0.051(8)			4851.1	0.026(10)
3728.4	5597.9(1)	5597.9	0.078(10)	3229.4	6096.9(5)	4867.2	0.028(10)
3712.7	5613.6(2)	5613.6	0.045(7)	3225.0	6101.3(3)	6101.3	0.026(7)
3695.8	5630.5(2)	5630.5	0.030(7)	3204.7	6121.6(3)	6121.6	0.029(7)
		3872.2	0.023(7)	3180.5	6145.8(2)	6145.8	0.054(10)
		3587.6	0.014(3)	3172.6	6153.7(5)	4924.0	0.034(11)
3655.0	5671.3(4)	5671.3	0.013(5)	3168.0	6158.3(2)	4928.6	0.067(13)
3634.0	5692.3(5)	4462.6	0.021(8)	3150.4	6175.9(6)	4946.2	0.028(11)
3614.1	5712.2(1)	5712.2	0.077(10)	3142.6	6183.7(2)	6183.7	0.061(10)

Table 1. (cont.)

E_1	E_i	E_2	$i_{\gamma\gamma}$	E_1	E_i	E_2	$i_{\gamma\gamma}$
3135.9	6190.4(5)	6190.4	0.014(5)	2658.1	6668.2(4)	4265.0	0.024(8)
3123.1	6203.2(3)	6203.2	0.032(7)	2640.1	6686.2(1)	6686.2	0.107(15)
3113.0	6213.3(3)	6213.3	0.026(7)	2623.3	6703.0(5)	5473.3	0.028(10)
3083.6	6242.7(3)	6242.7	0.019(5)	2612.9	6713.4(6)	6713.4	0.045(10)
3073.6	6252.7(1)	6252.7	0.061(10)			5483.7	0.035(10)
3066.0	6260.3(2)	6260.3	0.038(8)	2609.1	6717.2(4)	6717.2	0.024(7)
3059.2	6267.1(5)	4224.2	0.011(4)	2603.8	6722.5(4)	6722.5	0.016(5)
3054.0	6272.3(4)	6272.3	0.016(5)	2589.9	6736.4(4)	6736.4	0.016(5)
3044.4	6281.9(1)	6281.9	0.021(8)	2581.6	6744.7(4)	5515.0	0.028(8)
		5052.2	0.050(13)	2574.4	6751.9(5)	4426.0	0.025(10)
3041.6	6284.7(3)	6284.7	0.029(8)	2566.2	6760.1(5)	6760.1	0.013(5)
3029.2	6297.1(3)	6297.1	0.021(7)	2562.3	6764.0(4)	6764.0	0.018(5)
3021.7	6304.6(1)	6304.6	0.038(8)	2551.0	6775.3(12)	6775.3	0.021(5)
		4261.7	0.050(6)			4449.4	0.031(10)
2998.1	6328.2(3)	4285.3	0.018(4)	2538.9	6787.4(4)	6787.4	0.014(5)
2992.7	6333.6(4)	6333.6	0.029(7)	2533.2	6793.1(4)	6793.1	0.030(7)
		5103.9	0.037(11)			4750.2	0.011(3)
2982.2	6344.1(2)	6344.1	0.046(8)	2526.0	6800.3(5)	6800.3	0.013(5)
2968.6	6357.7(2)	6357.7	0.038(8)	2522.0	6804.3(4)	6804.3	0.018(5)
2961.7	6364.6(12)	6364.6	0.059(10)	2500.6	6825.7(4)	6825.7	0.024(7)
		4606.3	0.034(8)			5596.0	0.035(8)
2951.7	6374.6(3)	6374.6	0.035(8)	2497.5	6828.8(6)	5599.1	0.020(8)
2947.9	6378.4(5)	6378.4	0.018(7)	2463.7	6862.6(2)	6862.6	0.038(7)
2941.6	6384.7(3)	6384.7	0.034(7)	2445.8	6880.5(3)	6880.5	0.024(5)
2937.4	6388.9(4)	6388.9	0.021(7)	2432.0	6894.3(6)	6894.3	0.013(5)
2921.8	6404.5(6)	6404.5	0.011(5)			5664.6	0.018(8)
2906.1	6420.2(10)	5190.5	0.040(10)	2416.6	6909.7(3)	6909.7	0.014(5)
		4377.3	0.011(4)	2402.2	6924.1(5)	5694.4	0.018(7)
2897.4	6428.9(4)	6428.9	0.027(8)	2394.4	6931.9(3)	5702.2	0.028(7)
2890.7	6435.6(4)	4392.7	0.012(4)	2382.2	6944.1(11)	6944.1	0.010(5)
2888.1	6438.2(3)	4679.9	0.030(8)			4618.2	0.027(9)
2885.5	6440.8(4)	6440.8	0.035(10)	2345.0	6981.3(5)	6981.3	0.010(4)
2878.7	6447.6(3)	6447.6	0.035(10)	2339.4	6986.9(3)	6986.9	0.016(5)
2873.0	6453.3(8)	6453.3	0.026(8)	2333.4	6992.9(1)	6992.9	0.029(7)
		5223.6	0.058(11)			5763.2	0.021(7)
2867.6	6458.7(4)	5229.0	0.034(10)	2329.9	6996.4(3)	4670.5	0.034(9)
2840.9	6485.4(3)	6485.4	0.027(7)	2315.2	7011.1(3)	7011.1	0.018(5)
2829.1	6497.2(3)	6497.2	0.021(7)	2312.3	7014.0(3)	4276.0	0.042(10)
2824.5	6501.8(4)	6501.8	0.016(5)	2306.8	7019.5(3)	7019.5	0.030(7)
2817.3	6509.0(3)	4466.1	0.013(4)	2296.0	7030.3(5)	7030.3	0.010(5)
2810.6	6515.7(4)	6515.7	0.026(7)	2270.0	7056.3(4)	7056.3	0.016(5)
		5286.0	0.026(10)	2251.6	7074.7(2)	7074.7	0.026(7)
2799.6	6526.7(4)	6526.7	0.013(5)	2223.7	7102.6(3)	7102.6	0.013(4)
2792.9	6533.4(5)	6533.4	0.026(7)			5872.9	0.026(7)
		5303.7	0.029(10)	2214.9	7111.4(8)	7111.4	0.018(5)
2788.1	6538.2(5)	6538.2	0.013(5)			4785.5	0.041(8)
2770.6	6555.7(5)	6555.7	0.016(5)	2211.1	7115.2(4)	7115.2	0.011(4)
2766.9	6559.4(3)	6559.4	0.035(8)	2191.1	7135.2(3)	7135.2	0.013(4)
2762.5	6563.8(5)	6563.8	0.016(5)	2179.0	7147.3(3)	7147.3	0.018(5)
2753.3	6573.0(2)	6573.0	0.030(7)	2164.9	7161.4(3)	7161.4	0.014(5)
2745.1	6581.2(4)	4538.3	0.011(4)	2151.2	7175.1(6)	7175.1	0.010(4)
2727.7	6598.6(3)	6598.6	0.046(12)	2144.1	7182.2(2)	7182.2	0.027(7)
2725.1	6601.2(4)	6601.2	0.038(12)	2135.0	7191.3(3)	7191.3	0.018(5)
2704.4	6621.9(2)	6621.9	0.032(7)	2127.3	7199.0(3)	5156.1	0.010(3)
2694.6	6631.7(5)	5402.0	0.026(10)	2112.1	7214.2(5)	7214.2	0.010(4)
2680.0	6646.3(2)	5416.6	0.067(11)	2107.9	7218.4(4)	7218.4	0.014(5)

Table 1. (cont.)

E_1	E_i	E_2	$i_{\gamma\gamma}$	E_1	E_i	E_2	$i_{\gamma\gamma}$
2098.9	7227.4(4)	7227.4	0.013(5)	1877.9	7448.4(4)	7448.4	0.011(4)
2094.1	7232.2(2)	7232.2	0.022(5)	1850.2	7476.1(3)	5717.8	0.022(6)
2073.3	7253.0(3)	7253.0	0.026(5)	1834.6	7491.7(4)	7491.7	0.010(4)
2068.6	7257.7(2)	7257.7	0.027(7)	1829.1	7497.2(4)	7497.2	0.013(4)
2063.6	7262.7(3)	7262.7	0.019(5)	1803.1	7523.2(4)	7523.2	0.011(4)
2031.5	7294.8(4)	7294.8	0.014(5)	1797.6	7528.7(4)	7528.7	0.010(4)
2016.4	7309.9(4)	7309.9	0.014(5)	1771.2	7555.1(3)	5796.8	0.019(6)
1986.9	7339.4(5)	7339.4	0.010(4)	1767.8	7558.5(4)	7558.5	0.010(4)
1980.4	7345.9(2)	7345.9	0.016(5)	1731.1	7595.2(3)	7595.2	0.013(4)
1973.2	7353.1(3)	5027.2	0.023(7)	1707.6	7618.7(2)	5292.8	0.038(7)
1962.8	7363.5(4)	7363.5	0.014(4)	1690.3	7636.0(1)	5310.1	0.058(7)
		6133.8	0.023(7)	1674.1	7652.2(3)	4914.2	0.030(9)
		5605.2	0.018(6)	1447.5	7878.8(3)	7878.8	0.010(4)
1953.5	7372.8(4)	6143.1	0.020(7)	1198.0	8128.3(3)	8128.3	0.006(2)
1928.7	7397.6(3)	7397.6	0.011(4)	1166.4	8159.9(1)	6117.0	0.026(4)
1892.4	7433.9(3)	7433.9	0.013(4)				

1. The lower estimation of $i_{\gamma\gamma}$ for cascades with $E_1 < 520$ keV or $E_2 < 520$ keV.
2. Only statistical uncertainty of determination of energy and intensity.

3. Decay scheme

Two-step cascades following neutron capture unambiguously set energies of the initial and final levels but do not contain direct information on the energy of the intermediate level. However, if a cascade is of high intensity ($i_{\gamma\gamma} \geq 10^{-4}$ events per decay), then it is usually observed as a pair of well resolved peaks, and one can determine the ordering of emissions.

The method of construction of a decay scheme using the obvious relation about the constancy of the energy $E_1 = S_n - E_i$ of the primary transition in the cascades with different total energies $E_1 + E_2 = S_n - E_f = const$ was described for the first time in Ref. [3]. The method uses the multi-dimensional Gaussian distribution in the framework of the maximum likelihood method in order to select probable γ-transitions with equal energy in different spectra. As it was shown in Ref. [4], the algorithm gives reliable results even at the mean error $\simeq 1$ keV in the determination of the transition energies for some hundreds of cascades found in the decay scheme. The methods has been applied to analyse the measured spectra due to two-step cascades in slow-neutron capture in ^{117}Sn, and the result for the decay scheme for ^{118}Sn is given in Table 1.

Relative intensities of the most intense cascades of all 8 spectra obtained in the experiment were transformed into absolute intensities by normalization to the absolute intensities of their primary transitions [5] (Table 2). The branching ratios were obtained in the usual way from the numbers of coincidences accumulated in the experiment. Using the maximal number of the most intense cascades in the normalization procedure decreases its uncertainty due to the correlations between them. An estimate of the values of the statistical and systematic errors is given by a comparison of the sum of intensities of all cascades proceeding via the same intermediate level with the experimental intensity of their primary transitions. If

systematic errors in the determination of the cascade intensities are not present, the ratio $R = \sum i_{\gamma\gamma}/i_1$ should decrease when E_1 decreases. Values of R exceeding unity give some estimate of the total uncertainties for both intensities. Besides, owing to sufficiently different backgrounds in the spectra of cascade transitions and single γ-transitions, contribution of systematic error of i_1 in this uncertainty is larger than that of $i_{\gamma\gamma}$, at least for the primary transition with the smallest E_1.

The total absolute intensities $I_{\gamma\gamma} = \sum i_{\gamma\gamma}$ of cascades with a fixed sum energy (including those unresolved experimentally) obtained in this way at the detection threshold of quanta $E_\gamma > 520$ keV are listed in Table 3. Here the energy interval of the cascade final levels E_f is limited by conditions of the experiment – at the higher energies E_f, the peak/background ratio in the sum coincidence spectrum decreases. This does not allow one to get reliable information on the function $i_{\gamma\gamma} = f(E_1)$ for $E_f > 2 - 3$ MeV without the use of the Compton-suppressed spectrometer.

TABLE 2. The energies E_1 and absolute intensities (% per decay) i_1 of the most intense transitions used for normalization of the cascade intensities in ^{118}Sn. $\sum i_{\gamma\gamma}$ is the observed intensity of the cascades with corresponding primary transition.

E_1, keV	i_1 [5]	$\sum i_{\gamma\gamma}$
8096.37(17)	0.23(3)	0.37(2)
7268.84(13)	0.40(3)	0.44(1)
6997.7(4)	0.37(8)	0.31(2)
6648.52(7)	1.00(6)	0.75(3)
6422.14(11)	1.04(9)	0.88(4)
6110.0(2)	0.99(2)	0.80(3)
6055.66(18)	0.52(2)	0.55(3)
5444.9(3)	0.55(7)	0.35(1)
5298.1(5)	0.33(5)	0.28(1)
5217.51(10)	0.95(6)	0.60(3)
5208.7(2)	1.1(1)	1.09(4)
4781.55(16)	0.79(6)	0.28(2)
4765.99(15)	0.80(5)	0.51(3)
4556.31(14)	1.33(6)	0.39(4)
Sum	9.85(21)	7.6(1)

The total intensities $I_{\gamma\gamma}$ reveal serious deviations of the model values for the level density and radiative strength functions from the experimental results. Results of the calculation of $I_{\gamma\gamma}^{\rm mod}$ with the use of the level density model [6] and the model of radiative strength functions [7] for E1-transitions and strength function k(M1)=const are also listed in Table 3. The values of the experimental cascade intensities exceed considerably the calculated values. That means that the level density of really excited states after the thermal neutron capture is smaller than

that of predictions of the model in Ref. [6] and, probably, that the radiative strength functions of the primary transitions have a stronger energy dependence than that predicted by the model of Ref. [7].

TABLE 3. Energies $E_1 + E_2$ of cascades and their absolute intensities $I_{\gamma\gamma}$ (% per decay). E_f is the energy of the cascade final level.

$E_1 + E_2$, keV	E_f, keV	$I_{\gamma\gamma}^{\rm exp}$	$I_{\gamma\gamma}^{\rm mod}$
9326.30	0	16.0(34)	6.7
8096.63	1230	15.3(11)	7.2
7568.00	1758	2.4(7)	1.1
7283.42	2042	3.3(16)	2.4
7269.39	2057	2.8(9)	0.8
7000.36	2325+2328	5.6(9)	2.8
6923.08	2403	2.8(2)	1.5
6829.42	2497	[2]	0.5
6648.95	2677	[1.5]	1.0
6588.29	2738	[4]	1.7
sum		55.8(43)	25.7

Note: intensity of the cascades to the levels E_f = 2497, 2677 and 2738 keV was estimated from a comparison of their peak areas in the sum coincidence spectrum with the peak area corresponding to the cascades to the levels 2325 and 2328 keV.

3.1. Comparison with a known decay scheme

The decay scheme of ^{118}Sn achieved in this measurement includes 453 two-step cascades proceeding via 303 intermediate levels with the excitation energy up to $\simeq S_n - 1$ MeV; among those, 110 levels are depopulated by two or more secondary transitions. The reality of these levels is confirmed with a high confidence. (The mean uncertainty in the determination of the energy of the cascade quanta is 0.48 keV). Quanta ordering for 191 cascades cannot be determined within the algorithm of Ref. [3] because the corresponding intermediate levels are depopulated only by one secondary transition. Generally, many of these cascades can have a primary transition with a lower energy than the energy of the secondary transition. Quanta ordering in these 191 cascades was determined using the data from the ENDS file [8] on the decay scheme of the nucleus under study.

However, it should be noted that the levels at 2120, 2577 and 2725 keV listed in the ENDS file were not observed in our experiment, neither in the sum coincidence spectrum nor as intermediate levels of the cascades. Therefore, when using the data of Ref. [8], one should take into account that the estimated decay scheme can contain wrong levels and spin values at energies of the present measurement and at higher energy.

Neutron capture cross section in ^{117}Sn occurs through a single neutron resonance with the known parameters. Therefore, one can unambiguously assign spin and parity $J^\pi = 1^+$ to the compound state of ^{118}Sn formed in the capture. So, the levels of this nucleus excited by primary transitions after the capture (see Table 1) have, most probably, both positive and negative parity, and spin values in the interval $0-2$. The absence of the peak corresponding to the registration of the two-step cascades to level $E_f = 2280$ keV, $J^\pi = 4^+$ [8], in the sum-coincidence spectrum shows that, as in nuclei studied earlier, the total intensity of cascades with one purely quadrupole transition in ^{118}Sn is lower than the detection threshold of the experiment.

3.2. Fluctuations of the cascade intensities and problem of completeness of the decay scheme

According to the conventional notions, partial widths of primary transitions following neutron resonance capture in a non-magic nucleus have random values whose fluctuations with respect to the average obey the Porter-Thomas distribution [9]. This notion was not verified both for primary γ-transitions to the levels at excitation energy of several MeV and in the region of the smallest partial widths. Therefore, non-Gaussian character of the distribution of some amplitudes of the primary γ-transitions of a given multipolarity cannot be excluded. This could be due to the contribution of large components of the wave function of the levels connected by the corresponding transition in the matrix element of the primary γ-transition. In this case, experimental distribution of small partial widths will have smaller probability than what follows from the model of Ref. [9] owing to the violation of the condition of application of the central limit theorem of mathematical statistics.

The need for a practical solution of this question arises in the analysis of experimental data on the cascade intensities. Very low and rather even background in the intensity distributions of the cascades to the lowest levels of the studied nucleus provides better sensitivity of the coincidence study than the traditional experiment [5] with a single detector. This problem in the case of ^{118}Sn is more important than, for example, in deformed nuclei due to the larger number of intermediate levels which are depopulated only by γ-transitions with intensity exceeding the registration threshold.

The presence of 191 cascades of this kind and, therefore, the necessity to determine energies of their intermediate levels (without using the method of Ref. [3]) requires to solve the dilemma:

(a) either there are many levels at relatively low excitation energies in ^{118}Sn (for instance, $E_i < 3-4$ MeV) which do not manifest themselves in other reactions and, as a consequence, level density in this nucleus is noticeably higher than the predictions of the model of Ref. [6], at least, in this energy interval;

(b) or the number of primary transitions whose widths are $5-10$ times smaller

than the mean value is considerably smaller than what is expected according to Ref. [9] for the same excitation energy interval.

Considerably smaller threshold value of the function approximating the distribution for $E_{\mathrm{m}} > 5.5$ MeV in comparison with this parameter for lower energies admits only two these possible interpretations. This conclusion follows from Fig. 3 which represents comparison between the cumulative sums of the experimental in-

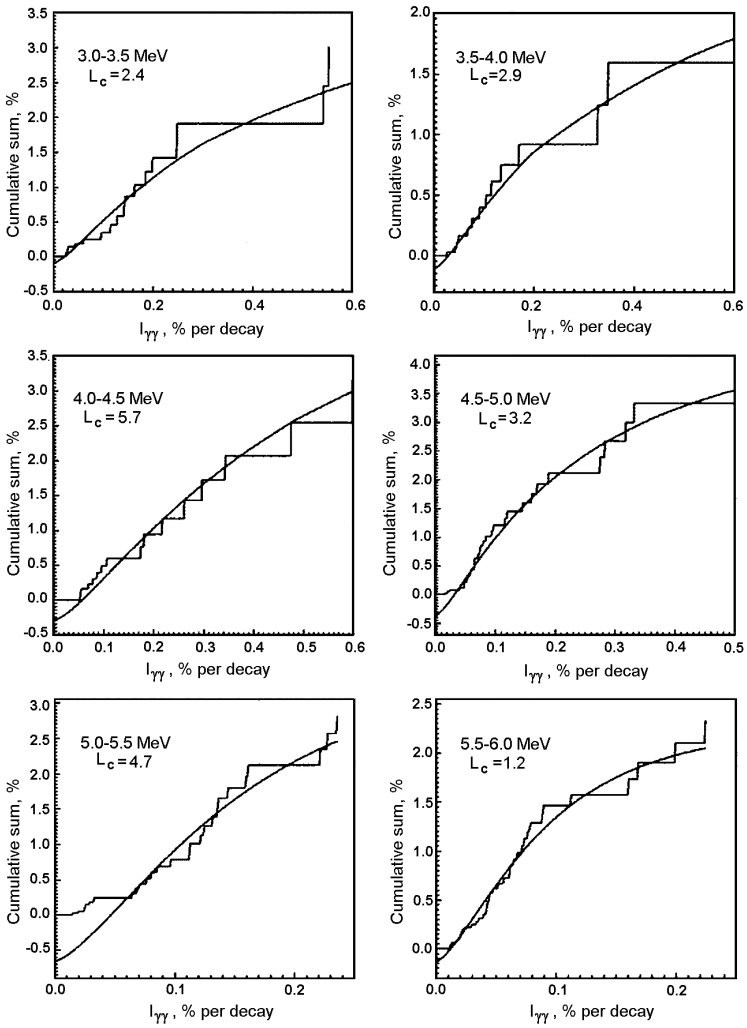

Fig. 3. Lines represent approximation and extrapolation of the cumulative intensities of cascades $i_{\gamma\gamma}$ (Table 1) in ^{118}Sn *for 6 energy intervals of their intermediate levels 3.0-3.5, 4.0-4.5, 4.5-5.0, 5.0-5.5, 5.5-6.0 and 6.0-6.5* MeV *versus intensity. Histogram represents the experiment. L_c is the approximated detection threshold (per* 10^4 *decays).*

tensities of cascades proceeding via the same intermediate level (for the energy bin $\Delta E_i = 0.5$ MeV) and corresponding approximation (as it was originally done in Ref. [10]). Experimental data in Fig. 3 were obtained under the condition that the low-intensity cascades were placed into the decay scheme in such a manner that their primary transitions have the lower energy. This assumption was used only if it was not possible to use to this aim the method of Ref. [3] or data on excited levels from Ref. [8].

4. Cascades with the low-energy primary γ-transitions

Fig. 2 represents a part of the experimental intensity distribution of the cascades to the ground state of ^{118}Sn. Decay scheme of this nucleus up to $E_{\rm ex} \geq 2.5$ MeV was very reliably established in other experiments. Based on all available data, one can state with a high confidence that this spectrum contains only 4 peaks due to the low-energy secondary transitions of the cascades in the interval 520 to 2500 keV [8]. The rest of the spectrum should be related to the registration of the cascades with the energies of primary transitions with $E_1 < 2.5$ MeV. A majority of the cascades with the high-energy primary transitions are usually registered as resolved intense peaks, and a number of low-intensity cascades with low-energy primary transitions form pseudo-continuous distribution in the spectrum.

The observation of the resolved peak related with registration of possible low-energy primary transition of the corresponding cascade permits one to get some information on the structure of the intermediate level of cascade. Intensity of individual cascade proceeding via a given intermediate level,

$$i_{\gamma\gamma} = i_1 \times i_2 \Big/ \sum i_2 \tag{1}$$

is always smaller than the intensity of its primary transition i_1 because the branching ratio $b_r = i_2 / \sum i_2$ cannot be greater than unity. Unfortunately, the background under the peaks in the sum-coincidence spectrum increases when the total energy of cascade $E_1 + E_2$ decreases. This makes impossible the extraction of the main part of the secondary transition intensities at the decay of any high-energy enough intermediate level and, as a consequence, to determine i_1 as a sum of all values $i_{\gamma\gamma}$ for a given intermediate level. But for some intense primary transitions, one can select from Ref. [5] a close energy γ-quantum (which in many cases was not placed into the decay scheme suggested by authors or was placed in such a manner that it was not observed in the corresponding distribution of the cascade intensities). Radiative strength functions determined for such cases can be compared with the predictions of the model of Ref. [7]. Analysis of the experimental intensity distributions $I_{\gamma\gamma}$ of two-step cascades to the ground and first excited states of ^{118}Sn [11] with accounting for the known total radiative width $\Gamma_\lambda = 80$ meV shows that the radiative strength function up to the energy $E_1 \simeq 3.5$ MeV does not exceed the value predicted by the model of Ref. [7]. Therefore, this model can be used for estimation of probability of low-energy primary transitions whose partial widths considerably exceed the mean value.

In this experiment, at least 15 cascades have been observed with the most intense, low-energy primary transitions ($E_1 < 2.5$ MeV) whose partial widths are at least 20 times larger than the prediction of Ref. [7]. According to the model of Ref. [6], approximately 26000 levels are expected to be excited by the primary $E1$ and $M1$ γ-transitions in the excitation energy region from 6.5 to 8.3 MeV. The probability to observe a random exceeding of partial width over the average value by a factor of 20 and more for the considered γ-transitions, calculated using the Porter-Thomas distribution, is equal to 10^{-5}.

Hence, from the above statement that some of the γ-transitions reported in Ref. [5] are really primary follows that some part of these transitions have anomalously large widths whose appearance cannot be random. Therefore, some of the levels with the excitation energy ≥ 6 MeV must considerably differ in the structure of the wave functions from those of the neighbouring levels, i.e., the effects like those observed at the low excitation energy manifest themselves also at higher excitations.

The presence of very intense low-energy primary γ-transitions was established earlier [12] in the ^{126,127,129,131}Te compound nuclei. They are interpreted as direct capture of neutron in the sub-shells $3p_{3/2}$ and $3p_{1/2}$. Unfortunately, clarifying of the structure of the considered levels of ^{118}Sn is impossible without further experimental and theoretical investigations.

5. Possible regularity of the excitation spectrum of intermediate levels of the most intense cascades

According to the modern theoretical notions, the wave-function structure of nuclear excited states is determined by a co-existence and interaction between the fermion (quasi-particles) and boson (phonons) excitations. With increasing excitation energy, a nucleus transits from practically mono-component excitations of the mentioned types to the mixed (quasi-particles $\otimes$ phonons) states with rather different degrees of their fragmentation [13]. This process should be investigated in details but there is no adequate experimental methods to study the structure of the wave functions at excitation energies exceeding 5 MeV.

Nevertheless, some information on the probable dominant components of the wave functions of heavy deformed nuclei can be obtained even in this case. The authors of Ref. [14] suggested to search for the regularity in the excitation spectra of the intermediate levels of most intense cascades by means of the auto-correlation analysis of the smoothed distributions of the sum-cascade intensities. The intensities presented in Table 1 were smoothed by means of the Gaussian function $F(E) = \sum i_{\gamma\gamma} \times \exp(-0.5(\Delta E/\sigma)^2)$. The distribution obtained using the parameter $\sigma = 25$ keV is given in Fig. 4, and the values of the auto-correlation function

$$A(T) = \sum_E F(E) \times F(E+T) \times F(E+2T) \tag{2}$$

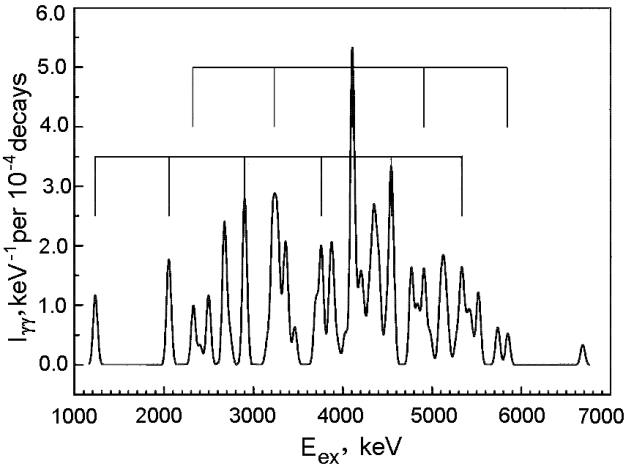

Fig. 4. The dependence of the "smoothed" intensities of resolved cascades listed in Table 1 on the excitation energy. Possible "bands" of practically harmonic excitations of the nucleus are marked. The parameter $\sigma = 25$ keV was used.

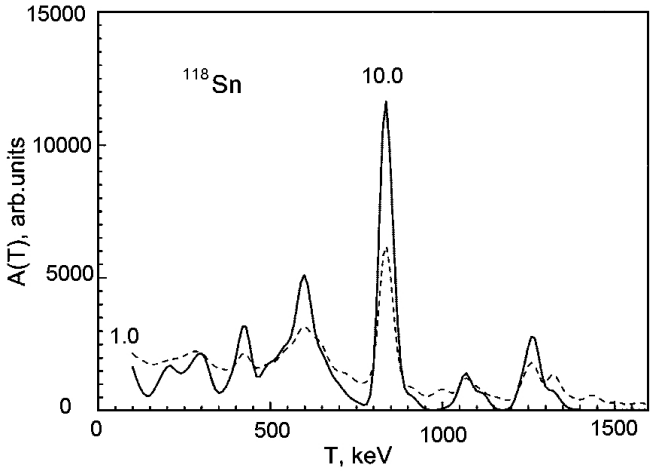

Fig. 5. The values of the functional $A(T)$ for two registration thresholds of most intense cascades. The value of the registration threshold (per 10^4 decays) is given in the figure.

for different selection thresholds of intense cascades are shown in Fig. 5. As was shown in Ref. [15], such analysis cannot give a unique value of the equidistant period T even for the simulated spectra (for example, for 25 "bands" consisting of 4 levels with slightly distorted equidistant period and intensities of cascades) and provide an estimation of the confidence level of the observed effect. In principle, both problems can be solved by measurements of the two-step cascades due to different resonances of the same nucleus. But some grounds to state that the regularity really exists can

be obtained from a comparison of the most probable equidistant periods in different nuclei. The set of the probable equidistant periods obtained so far (Fig. 6) allows the assumption that the T value is approximately proportional to the number of boson pairs in the unfilled nuclear shells. This allows one to consider the effect at the level of a working hypothesis, even though a finite probability of a random existence of a regularity of intermediate levels of the most intense cascades in a nucleus cannot be excluded.

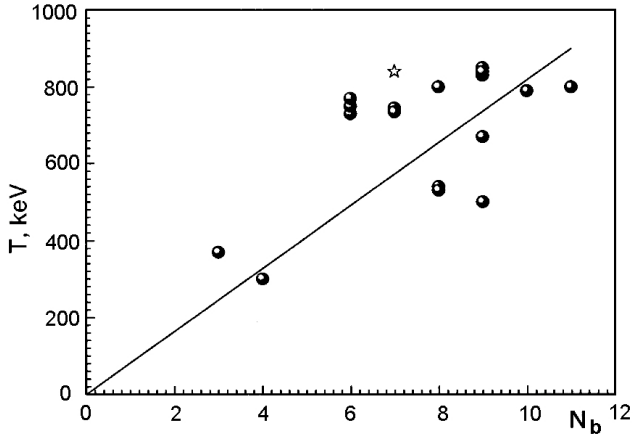

Fig. 6. The value of the equidistant period T for ^{118}Sn (asterisk) and other investigated even-even nuclei as a function of the number of boson pairs N_b in the unfilled shells. The line represents possible dependence (eyedrawn).

The regularity in the excitation spectra testifies to the harmonic nuclear vibrations. Thus, one can assume that the structure of the intermediate levels of the studied cascades contains a considerable components of rather weakly fragmented states, like multi-quasi-particle excitations $\otimes$ phonon or several phonons. This provides logical explanation of the serious decrease in the observed level density as compared with the predictions of the non-interacting Fermi-gas model: nuclear excitation energy concentrates on phonons, but quasi-particle states in the energy interval up to $\simeq 2$ MeV are excited weakly or very weakly due to insufficient energy for breaking up of paired nucleons. This seems to be a reasonable but probably not the only explanation.

6. Cascade population of levels in ^{118}Sn

Obvious deviations of the level density and radiative strength functions from predictions of the simplest models like those of Refs. [6[and [7], and the probable regularity in the excitation spectra of intermediate levels of the most intense cascades, show that our understanding of the cascade γ-decay process needs an improvement and some corrections. This follows from a comparison between the experimental and the model-calculated values of the population of the high-lying

levels of the nucleus under study. It is seen from Eq. (1) that using reliable information on the intensities of individual cascades and known intensities of their primary and secondary transitions [5], one can determine $\sum i_2$, which equals the total population of a given level by the direct primary transitions and any possible cascades.

One can subtract the primary transition intensity from this value in order to decrease its fluctuation. The populations obtained in this manner for the levels with positive parity are compared with the model-calculated values in Fig. 7. It should be noted that the difference between the calculated populations of levels with the same spin but different parities is insignificant. It is seen that the correspondence between the experiment and calculation for the levels above ≈ 3 MeV cannot be achieved. This result confirms the conclusion made above on the presence of the intervals of excitation-energy at which occur large changes in the properties of the excited states of deformed and also of spherical nuclei. On the other side, it points at the necessity to develop better nuclear models for the full interval of the excitation energies up to $E_{\rm m} \simeq S_n$.

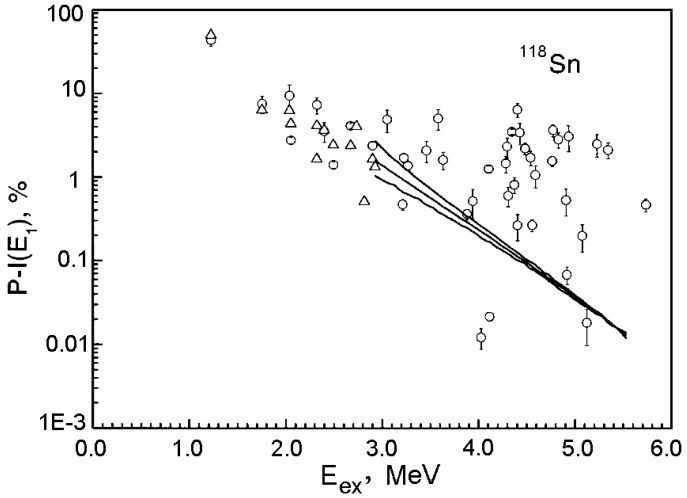

Fig. 7. Experimental population of different levels in ^{118}Sn *(points with bars) in comparison with that calculated for levels* $J^\pi = 0^+, 1^+, 2^+$ *within models [6] and [7] using* $k(M1) = const$ *- curves and triangles.*

7. Conclusion

This article presents the first large enough and reliable scheme of excited states of the ^{118}Sn compound nucleus and of modes of their decay up to the excitation energy of more than 3 MeV, obtained in the measurements of two-step cascades following the neutron capture in ^{117}Sn nuclei.

Analysis of the data shows, in particular, that an improvement of the descrip-

tion of properties of spherical nuclei is needed for a more detailed accounting of the co-existence and interaction of quasi-particle and phonon components of wave functions of the levels excited after the neutron capture.

Acknowledgements

This work was supported by GACR under contract No. 202/03/0891 and by RFBR Grant No. 99-02-17863.

References

[1] J. Honzátko et al., Nucl. Instr. Meth. **A376** (1996) 434.

[2] A. M. Sukhovoj and V. A. Khitrov, Sov. J.: Prib. Tekhn. Eksp. **5** (1984) 27.

[3] Yu. P. Popov, A. M. Sukhovoj, V. A. Khitrov and Yu. S. Yazvitsky, Izv. AN SSSR, Ser. Fiz. **48** (1984) 1830.

[4] S. T. Boneva, E. V. Vasilieva and A. M. Sukhovoj, Izv. RAN., Ser. Fiz., **51(11)** (1989) 2023.

[5] Yu. E. Loginov, L. M. Smotritskij, P. A. Sushkov, Vopr. Atom. Nauki i Tech., ser. Fiz. Yad. Reac. (in Russian), **1/2** (2001) 72.

[6] W. Dilg, W. Schantl, H. Vonach and M. Uhl, Nucl. Phys. **A217** (1973) 269.

[7] S. G. Kadmenskij, V. P. Markushev and W. I. Furman, Sov. J. Nucl. Phys. **37** (1983) 165.

[8] K. Kitao, Nucl. Data Sheets, **75(1)** (1995) 99; http://www.nndc.bnl.gov/nndc/nsr/nsrframe.html.

[9] C. F. Porter and R. G. Thomas, Phys. Rev. 1956. **104** (1956) 483.

[10] A. M. Sukhovoj and V. A. Khitrov, Physics of Atomic Nuclei, **62(1)** (1999) 19.

[11] E. V. Vasilieva, A. M.Sukhovoj and V. A. Khitrov, Physics of Atomic Nuclei, **64(2)** (2001) 153.

[12] I. Tomandl, V. Bondarenko, D. Bucurescu, J. Honzátko, T. von Egidy, H.-F. Wirth, G. Graw, R. Hertenberger, A. Metz and Y. Eiserman, *Proc. 10 Int. Symp. Capture γ-Ray Spectroscopy and Related Topics, Santa Fe, U.S.A.*, Ed. by S. Wender, AIP (1999) 200.

[13] L. A. Malov and V. G. Soloviev, Yad. Fiz. **26(4)** (1977) 729.

[14] A. M. Sukhovoj and V. A. Khitrov, Bull. Russian Acad. Sci., Physics **61(11)** (1997) 1611.

[15] E. V. Vasilieva et al., Bull. Russian Acad. Sci., Physics **57** (1993) 1582.

JAKE DVOJNE KASKADE I SHEMA γ-RASPADA SLOŽENE JEZGE ^{118}Sn

Mjerili smo energije i intenzitete 453 dvojne kaskada koje slijede uhvat termalnih neutrona u ^{117}Sn. Podaci su omogućili određivanje znatno proširenje ranije sheme raspada jezgri ^{118}Sn i točnije rezultate. Analiza autokorelacije uzbudnog spektra međustanja najjačih kaskada omogućila je određivanje vjerojatne periodičnosti. Pokazuje se da nije moguće kvantitativno objasniti ukupne jakosti kaskada ako se uzmu u obzir samo fermionske uzbude. Zaključuje se da vibracijske uzbude znatno utječu na γ-raspade u ^{118}Sn sve do energije odvajanja neutrona S_n.